General Disclaimer

One or more of the Following Statements may affect this Document

- This document has been reproduced from the best copy furnished by the organizational source. It is being released in the interest of making available as much information as possible.

- This document may contain data, which exceeds the sheet parameters. It was furnished in this condition by the organizational source and is the best copy available.

- This document may contain tone-on-tone or color graphs, charts and/or pictures, which have been reproduced in black and white.

- This document is paginated as submitted by the original source.

- Portions of this document are not fully legible due to the historical nature of some of the material. However, it is the best reproduction available from the original submission.

SQT

ICASE

COMPUTATION OF ACOUSTIC WAVES IN A JET

A. Bayliss

and

E. Turkel

Report No. 78-22
December 22, 1978

INSTITUTE FOR COMPUTER APPLICATIONS IN SCIENCE AND ENGINEERING
NASA Langley Research Center, Hampton, Virginia

Operated by the

UNIVERSITIES SPACE USRA RESEARCH ASSOCIATION

COMPUTATION OF ACOUSTIC WAVES IN A JET

Alvin Bayliss
Institute for Computer Applications in Science and Engineering

and

Eli Turkel
Courant Institute of Mathematical Sciences
New York University

ABSTRACT

A numerical treatment of acoustic waves in a jet is described. The full time dependent Euler equations are used in both linear and nonlinear formulations. The computational region of integration is artificially bounded and boundary conditions are developed to simulate outgoing waves and to enable the computational domain to be substantially restricted. Higher order methods and coordinate transformations are introduced to further reduce the number of grid points as well as to increase the efficiency of the program. Numerical results are presented for time harmonic sources as well as for sources with more complicated time dependence.

The first author was supported under NASA Contract No. NAS1-14101 while in residence at ICASE, NASA Langley Research Center, Hampton, Virginia. The research for the second author was partially supported under the United States Air Force Office of Scientific Research Contract AFOSR-76-2881 and NASA Contract No. NAS1-14101.

Introduction

This study is concerned with the numerical computation of time dependent acoustic waves in a jet. The presence of inhomogeneities causes a significant change in acoustic behavior and aero-acoustic noise prediction schemes must take this into account in order to accurately predict aerodynamic noise. We will be concerned here only with the propagation of sound and not with its generation. Thus the acoustic sources will be modelled by arbitrary forcing terms in the equations.

Previous workers (Schubert [1], Liu and Maestrello [2], Mungur et al. [3]) have approached the problem by deriving a convective wave equation for the pressure and then assuming that both the source and the solution have a time dependence of the form $e^{i\omega t}$. The use of this assumption in the convective wave equation leads to an elliptic equation for the acoustic pressure. In the case of zero mean flow this elliptic equation is the Helmholtz equation.

A very efficient solution method for the elliptic equation was introduced by Schubert [1]. He split the linear elliptic equation into two coupled nonlinear equations for the amplitude and phase of the time dependent solution. A motivation for this approach is that these quantities are smoother than the pressure and so can be efficiently approximated on a coarse grid.

The method used here differs from the above approach in two ways. First the time dependent equations are used rather than assuming a time harmonic behavior. This is because there are physical problems of interest where the source does not have a simple time harmonic dependence. For example, in a real jet the sources generally are convected downstream with the jet. Other sources of interest are those which have a pulse type time

dependence. Numerical results for these types of sources will be presented here.

A second difference from previous work is that in the present study the first order equations of fluid dynamics are integrated. There are several limitations in the use of a convective wave equation for the pressure. The primary one is that several physical approximations are necessary in order to eliminate the acoustic velocities (see [1]). These assumptions are generally of the type that the wave length of the sound is small compared with the diameter of the jet. Since only relatively low frequencies can be computed numerically the validity of these approximations is open to question. Furthermore, the exclusion of the velocities in the convective wave equation complicates the boundary conditions needed to simulate outgoing waves. Third the nature of the source term is less clearly defined than in the primitive equations of motion. For example, a source of mass or momentum can be easily included in the primitive equations but does not correspond to any simple type of source in the convective wave equation. On the other hand the primitive equations can be easily modified to include nonlinear effects that are neglected in the standard linearizations. Finally explicit finite difference schemes, which are ideal for vector machines as the STAR-100, can be applied to yield very efficient algorithms.

The computational effort required to solve the first-order system is not substantially greater than that required for the convective wave equation. The second order wave equation requires at least two levels of storage while the first order system can be programmed with one level of storage for each of the unknowns. When the source has a harmonic time dependence then the time dependent procedure can be considered as

an iteration scheme to obtain the time harmonic solution. In this case further study is required to determine if this approach is competitive with the multi-grid methods used by Fix, Gunzburger, and Nicolaides [4].

The present method requires computational resolution of the solution on the basis of the wavelength. This will also be true of any method that solves the time independent equations, either as a first order system or as a single second order equation. Such methods can not generate accurate solutions using grids as coarse as those used by Schubert. Indeed, the authors have found that a substantial fraction of the total number of points used by Schubert is required merely to resolve the mean flow of the jet.

The method of Schubert requires essentially that the solution be composed of only one wave. If we define a wave as a function of the form

$$w(\vec{r}) = A(\vec{r})e^{ikS(\vec{r})} \quad .$$

where A and S are slowly varying real valued functions of the spatial point $\vec{r}$, and k is the wave number, then A and S can be approximated with a coarser grid than the solution w. However, the assumption that the solution be composed of only one wave is a very restrictive assumption which in general does not hold. For example, if the jet exits from a wall there will be reflections off the wall which will introduce other waves. Our results indicate that even for the problem considered by Schubert reflections occur because of the gradient of the mean flow. The method presented here permits the accurate computation of these cases but is restricted in the frequency range for which it can be applied.

II. Equations

The equations of motion for an inviscid axially symmetric flow in cylindrical coordinates are

$$\rho_t + (\rho u)_z + (\rho v)_r + \frac{\rho v}{r} = 0$$

$$u_t + uu_z + vu_r + \frac{p_z}{\rho} = 0 \tag{2.1}$$

$$v_t + uv_z + vv_r + \frac{p_r}{\rho} = 0 \ .$$

ρ is the density, u and v are the axial and radial components of velocity respectively and p is the pressure. We assume an isentropic flow so that

$$p = A\rho^{\gamma} \tag{2.2}$$

where A is a constant. These equations are to be integrated for $t > 0$ and for all space $r > 0$, $-\infty < z < \infty$. In addition, we need to introduce additional terms into (2.1) to simulate the acoustic sources.

In order to incorporate properties of the mean flow we expand the solution about the mean flow of the jet $(\rho_0, u_0, v_0)^T$.

$$\begin{pmatrix} \rho \\ u \\ v \end{pmatrix} = \begin{pmatrix} \rho_0 \\ u_0 \\ v_0 \end{pmatrix} + \varepsilon \begin{pmatrix} \rho' \\ u' \\ v' \end{pmatrix} \tag{2.3}$$

where ε is a perturbation parameter determining the amplitude of the source. The acoustic approximation generally assumes ε is small. In addition we non-dimensionalize the system by choosing new variables

$$\bar{t} = \frac{ta}{d} \qquad \bar{z} = \frac{z}{d} \qquad \bar{r} = \frac{r}{d}$$

$$\bar{\rho} = \frac{\rho}{\rho_\infty} \qquad \bar{p} = \frac{p}{p_\infty} \qquad \bar{u} = \frac{u}{a} \qquad \bar{v} = \frac{v}{a}$$

where d is the diameter of the jet, a is the ambient sound speed and p_∞, ρ_∞ are the ambient pressure and density respectively. For simplicity we will drop the bars in the sequeal; all quantities will be non-dimensionalized.

The mean flow for the jet was obtained from experimental data (Maestrello [5]) which indicates that p_0 is nearly constant and v_0 is, in the extreme case, only about 2 percent of u_0. Computational experience confirms that the inclusion of v_0 makes little difference. Hence, for the remainder of this study we neglect v_0 and assume that p_0 is constant (p_∞). The mean velocity u_0 corresponds to a spreading jet with a spread of about 12°. For fixed z the mean flow has a maximum at the axis and decays with distance normal to the axis. Further details of this flow can be found in [5].

In order to facilitate the comparison of linear and nonlinear models we introduce new variables

$$\begin{aligned} \tilde{\rho} &= \rho' \\ \tilde{u} &= (1+\varepsilon\tilde{\rho})u' \\ \tilde{v} &= (1+\varepsilon\tilde{\rho})v' \\ \tilde{p} &= ((1+\varepsilon\tilde{\rho})^{\gamma}-1)/\varepsilon. \end{aligned} \tag{2.4}$$

For non-zero ε the quantities $\tilde{u}$ and $\tilde{v}$ are part of the terms making up the non-dimensionalized momenta. The choice of dependent variables in (2.4) puts the resultant system of equations in conservation form. Upon

including a source term in the mass equation of (2.1). We can rewrite (2.1) as

$$\tilde{\rho}_t + (\tilde{\rho}u_0 + \tilde{u})_z + (\tilde{\rho}v_0 + \tilde{v})_r + \frac{\tilde{\rho}v_0 + \tilde{v}}{r} = F(z,r,t)$$

$$\text{(2.5)} \qquad \tilde{u}_t + [\tilde{u}(u_0+\varepsilon u')]_z + [\tilde{u}(v_0+\varepsilon v')]_r + \left[\frac{(1+\varepsilon\tilde{\rho})^\gamma}{\varepsilon\gamma}\right]_z = \tilde{u}v_{0,r} - \tilde{v}u_{0,r} + \varepsilon\tilde{u}(F + \frac{v'}{r})$$

$$\tilde{v}_t + [\tilde{v}(u_0+\varepsilon u')]_z + [\tilde{v}(v_0+\varepsilon v')]_r + \left[\frac{(1+\varepsilon\tilde{\rho})^\gamma}{\varepsilon\gamma}\right]_r = \tilde{v}v_{0,z} - \tilde{u}v_{0,z} + \varepsilon\tilde{v}(F + \frac{v'}{r})$$

$$0 < r < \infty, \qquad -\infty < z < \infty, \quad t > 0.$$

If ε is set to zero in (2.5) we obtain a linear system for the acoustic density and velocities. (The acoustic pressure is proportional to the acoustic density by linearizing (2.2)). For most of the study we have used the linearized equations, $\varepsilon = 0$. Differences between the linear and nonlinear equations are discussed in section 5.

Generally, we take the source as being of the form $F(z,r,t) = f(t)\delta(\sqrt{r^2+(z-z_0)^2})$ for some axial point z_0. The delta function source when implemented in the primitive equations of motion corresponds to a simple source of mass or momenta depending on which equation it is in. Axial dipoles and quadrapoles can also be handled easily. This is one of the advantages of working with the Euler equations. The delta function is modeled by a Gaussian centered at the source point. In previous work ([1], [2]) the source was modeled by excluding a small circular region from the domain of integration and then imposing suitable boundary conditions. This approach was originally used for this study but was discontinued as being inconvenient for optimized vector computation on the CDC STAR-100.

Equations (2.5) must be supplemented by initial and boundary conditions. The initial conditions specified are $\tilde{\rho}$, $\tilde{u}$, $\tilde{v} = 0$ at $t = 0$ (i.e. the source is switched on from a state of rest). Analytically the domain of integration is the entire plane; computationally we require a bounded domain with appropriate boundary conditions. This is treated in detail in section 4.

III. Numerical Scheme

The system (2.5) can be written in the general form

$$w_t + F_z + G_r = H . \tag{3.1}$$

We solve this system by splitting it into a sequence of one dimensional problems (see Strang [6], MacCormack [7]). Let L_z and L_r denote the finite difference approximations to the one-dimensional equations

$$w_t + F_z = H_1$$

$$w_t + G_r = H_2$$

respectively, where $H = H_1 + H_2$. Then, the solution to (3.1) is updated, with second order accuracy in time, by

$$w(t + 2\Delta t) = L_z L_r L_r L_z w(t). \tag{3.2}$$

The solution was found to be insensitive to the decomposition of H except that $\frac{v}{r}$ had to be included in L_r.

For the numerical operators L_z and L_r, a spatially fourth order accurate extension of the MacCormack method developed by Gottlieb and Turkel [8] was used. The higher order accuracy was necessary in order to efficiently compute the solution at large distances from the jet exit. The higher order formulas allow a greatly reduced mesh without any loss of accuracy as compared with second order methods. Detailed comparisons of second and fourth order methods are given by Turkel [9]. There it is shown that fourth order methods allow halving the mesh in each direction for a given error tolerance of about five percent. In addition the higher order method is about three times faster, to achieve comparable accuracy, as a second order scheme. In order to further reduce the number of mesh points an exponential coordinate stretching was introduced in both directions. This concentrates points near the axis and near the source. Finally at points where sufficient boundary conditions are not prescribed a third order extrapolation of the fluxes is used as described in [9].

The explicit nature of the fluxes F, G given by (2.5) allows their computation over the entire grid by vector operations. Hence, this algorithm is well-suited for a vector processor such as the STAR-100. The program was coded in 32 bit arithmetic in SL-1, a high level compiler written for the STAR. Including all factors, such as some recoding to facilitate vectorization, the program ran 80 times faster on the STAR than on a CYBER-175 serial computer.

IV. Boundary Conditions

For computational purposes the infinite domain of integration for (2.5) must be replaced by a bounded domain on which appropriate boundary conditions must be specified. Since the infinite space problem is well posed for the

hyperbolic system (2.5), it is necessary to develop radiation boundary conditions only to achieve accuracy and computational efficiency. In principle, for any finite region and for a fixed time of integration one can place the artificial boundaries sufficiently far away so that the numerical solution is accurate in the region of interest. This is not practical since, in fact, one needs to constrict the region of integration as much as possible, in order to reduce the number of grid points. Our experience indicates that this is the fundamental computational difficulty in obtaining accurate solutions to (2.5). All this is fundamentally different from the Helmholtz equation where a radiation condition is required to obtain a unique solution (cf. Hellwig [10]).

Two types of boundary conditions are required corresponding to inflow and outflow situations. Inflow conditions occur where the jet enters the region of interest while outflow conditions occur at the far field cutoff where outgoing waves must be simulated. A complete description and justification of these conditions is given by Bayliss and Turkel [11]. Here, a summary of the actual conditions, which were used in this study is presented.

A. Three types of inflow configurations are considered and are illustrated in figures 1-3. These figures are presented in cylindrical coordinates with axial symmetry understood. These inflow conditions are:

1. A semi-infinite pipe extending into free space (figure 1).

2. A semi-infinite pipe extending from an acoustic baffle (figure 2).

3. An anti-jet, that is a convergent upstream flow (figure 3). The anti-jet is obtained by reflecting the mean flow symmetrically about the plane of the nozzle exit.

Conditions 1 and 2 correspond to physically realistic situations. In both cases two conditions must be imposed at the pipe exit (dashed line in figures 1 and 2). We have indicated (dotted line in figure 1) an outflow boundary directly above the nozzle; also included are far field boundaries (indicated by ·——·). Experimentally, one is not interested in the acoustic field above the pipe even for case (1).

The anti-jet is a nonphysical, computational device introduced in the treatments of the convective wave equation in order to remove the necessity of specifying boundary conditons along the pipe and at the nozzle exit. These conditions are difficult to impose for the convective wave equation since the velocities are not independent variables. However, the anti-jet formulation has several disadvantages. Besides being nonphysical it requires the solution of the equations in a much larger region than necessary. Finally, at the inflow (left) boundary u_0 is positive over portions of the boundary. Hence, two boundary conditions must be specified in order to have a well posed problem. We have not succeeded in developing such an additional condition. For the computational results computed with the anti-jet this inflow boundary was sufficiently far away so that u_0 was small. Using only the radiation boundary condition (to be described) instability was delayed long enough to permit a periodic solution to be generated downstream. Clearly the use of the anti-jet is unsatisfactory and inefficient for time dependent equations. The anti-jet was used in this study for only a few test cases for comparison purposes. All other cases used either boundary conditions 1 or 2.

For the inflow pipe we assume a constant mean flow u_0 and $\varepsilon = 0$. We further assume that the flow is one dimensional, i.e. independent of

r. From characteristic theory one finds that the appropriate boundary conditions at the jet exit are

$$u + p = 0 \tag{4.1}$$

$$v = 0. \tag{4.2}$$

In [11] we present a justification for these conditions for the full two dimensional problem based on an expansion of modes travelling down the pipe; they help explain the numerical results presented in the next section. Rogers [12] has shown that these conditions imply that the energy flux through the pipe is negative, i.e., no energy flows from the pipe into the computational domain and hence (2.5) is well posed in the sense of Hadamard.

B. The outflow boundary conditions must approximate the condition for outgoing waves. The mean flow decays with the distance from the nozzle and when u_0 is zero (2.5) can be reduced to a wave equation for p. The condition for outgoing waves can then be expressed in terms of $\theta = \tan^{-1} \frac{r}{z}$ and $d = (r^2+z^2)^{\frac{1}{2}}$ by

$$p = \sum_{j=1}^{\infty} \frac{f(t-d,\theta)}{d^j} \tag{4.3}$$

(see [11] and also Friedlander [13]). This implies that

$$p_t + p_d = -\frac{p}{d} + O(\frac{1}{d^3}) \tag{4.4}$$

which upon using (2.5) with $u_0 = 0$, $\varepsilon = 0$ is equivalent to

$$u_t^d - p_t = \frac{p}{d} + 0\left(\frac{1}{d^3}\right) \tag{4.5}$$

where u^d denotes the radial velocity in polar coordinates. Although these equations are strictly valid only when $u_0 = 0$ exterior to some sphere, we have applied it to very constricted domains with substantial success, as is described in the next section. Computational experiments show that the correction $\frac{p}{d}$ in (4.5) is necessary in order to control false reflections at the boundary. The condition (4.5) is part of a family of boundary conditions asymptotic to any order in $\frac{1}{d}$ (see [11]).

The boundary condition (4.5) is coupled with cubic extrapolation on the fluxes for u and v as described in [9]. This enables us to solve for the variables on the boundary. Gottlieb, Gunzburger, and Turkel [14] demonstrate that numerical stability can be improved by use of characteristic variables for those quantitites which are not analytically prescribed. For the computations in this study it was never necessary to use characteristic variables. Instead, the radiation boundary condition (4.5) was used to calculate the pressure after the two equations for u and v had been integrated.

The radiation boundary conditions presented here differ from those introduced by Engquist and Majda [15]. Ours are asymptotic in the distance of the cutoff while the expansions of Engquist and Majda are asymptotic in the deviation of the wave from normal incidence. The conditions at the nozzle (4.1 - 4.2) are formally equivalent to the first order condition in [15], the justification for which is based on the constraint $v = 0$ in the pipe. An analysis of the appropriate equations shows that these conditions are rigorously asymptotic in the distance of the pipe for

frequencies below a fixed limit, which includes all frequencies for which numerical studies are feasible. This is discussed in detail in [11].

V. Numerical Results

The first computations were designed to test the boundary conditions described in the previous section. Computations were performed comparing the nozzle inflow conditions (4.1 - 4.2) with the anti-jet. Computations with different frequencies as well as computations with pulse type forcing functions all yielded virtually indistinguishable results for both sets of boundary conditions. Therefore, all the remaining results were produced for the configuration shown in figure 1. Here the outflow radiation conditions are imposed directly above the nozzle (dotted line in figure 1). This eliminates all upstream integrations.

We first consider a time harmonic source. Then the forcing function in (2.5) is given by

$$F(z,r,t) = H(t)\left[\cos \omega t\right]\left[\delta\left(\sqrt{r^2+(z-z_0)^2}\right)\right] \tag{5.1}$$

$H(t)$ is a smooth approximation to the Heaviside function and z_0 is 2 jet diameters upstream of the nozzle. The linearized equations, $\varepsilon = 0$, are solved.

The quantity of physical interest is the relative sound pressure level (SPL). Let $p(z,r,t)$ be the non-dimensionalized pressure in (2.5). We then define

$$I(z,r) = \left[\frac{2\int_0^T p^2(z,r,t)dt}{T}\right]^{\frac{1}{2}}. \tag{5.2}$$

This integral is taken over one period once a periodic oscillation has been established. If $\cos\omega t$ in (5.1) is replaced by $e^{i\omega t}$ and if we assume that

$$p(z,r,t) = e^{i\omega t}\,\hat{p}(z,r)$$

then it follows that

$$I(z,r) = |\hat{p}(z,r)|. \tag{5.3}$$

We then define

$$SPL = 20\,\log_{10} I(z,r). \tag{5.4}$$

This corresponds to the sound pressure level in the usual sense (see [1]). For general, nonharmonic problem the definition (5.2) is an extension of the definition of (SFL) provided T is chosen large enough. The pressure is usually normalized relative to some reference pressure p_0. Since only differences in SPL are important this normalization can be ignored. Differences between the SPL at different points are measured in decibels (d.b.).

For the first set of experiments we consider the harmonic source (5.1) with different boundary conditions. The figures 4-7 display the SPL, relative to 90°, at a fixed distance from the source and as a function of the angle θ. For these runs, unless otherwise stated, the exit Mach number is .62, the non-dimensional frequency is 1.145, and the downstream boundary is at 65 diameters from the source. The radial cutoff is denoted by R_T and is measured in jet diameters.

The fundamental physical effect to be expected here is the bending of sound waves away from the axis, a phenomena known as refraction. This results in a substantial reduction in the SPL as the axis is approached (i.e. $\theta \to 0$). This refraction effect decreases as $\theta \to 90^\circ$ so that the solution approaches the solution with no flow (i.e. the wave equation). This fact is used as a check on the code as well as a justification for constricting the computational domain to a narrow region around the jet axis.

Figure 4a and 4b show plots of the SPL for different values of R_T. When reference values at 90° are not available they are taken from the case with $R_T = 57$. It is clear that we can severely constrict the domain normal to the jet without seriously degrading the solution. The SPL is relatively insensitive to pointwise errors, however examination of the pointwise solution indicates very small errors due to the constriction of the region. This is also true if the downstream cutoff is decreased. If the lower order term p/d is dropped in the radiation boundary condition (4.5) then much larger regions are required to control the reflections from the boundary. The solutions presented here agree closely with those obtained in [2] near the axis. The increase in the SPL that is found at mid-angles was found in all the runs with the harmonic source. This was not found in previous studies, probably because of a lack of resolution in the angular direction.

In Figure 5 results are shown for the case of a jet exiting from an acoustic baffle. In this problem there is a reflected wave from the baffle and it is clear from the figure that at higher angles there is at first a cancellation due to the interference of the waves and then a reinforcement.

In Figure 6 comparisons are presented with experimental results of Grande (see [1]). We note that there is good qualitative agreement except that the rate of increase of the SPL is steeper as θ increases from zero. Comparisons with extensive experiments being conducted at NASA Langley Research Center will be presented subsequently.

Computations were made with the nonlinear equations (2.5) with different values of ε. Our results showed that the SPL level was largely unaffected by the nonlinear terms except in the near field where the axial dip was slightly reduced for $\varepsilon \sim .02$ (based on a nondimensional P_∞ of 1). For higher values of ε the scheme exhibited nonlinear instabilities which would require artificial dissipation to control.

The time dependent calculations with the harmonic forcing term indicated that secondary reflections from the gradient of the mean flow are present near the axis. To demonstrate this more clearly we present numerical computations with a pulse type solution. In this case the source in (2.5) is given by

$$F(z,r,t) = f(t)\delta\left(\sqrt{r^2+(z-z_0)^2}\right) \tag{5.5}$$

where $f(t)$ is a smooth approximation to a delta function.

In Figure 7 the pressure is plotted as a function of time, at a fixed axial point 20 diameters downstream of the source. Results are presented for four different values of the exit Mach number. The striking feature to observe is the strong secondary wave occuring after the primary wave. We have verfied that this is insensitive to numerical changes such as the position of the artificial boundaries and grid refinements.

The secondary wave is not a near field phenonmena and will occur at far field axial points over a sufficiently long time interval. The time of arrival of the secondary wave is inversely proportional to the exit Mach number while the amplitude is, to good approximation, proportional to the square of the Mach number.

As a third example we consider time-harmonic sources convecting down the axis of the jet. We consider a model where sources drift downstream of the jet for one diameter and then are recreated at their initial position. This represents a reasonable model for the convection of acoustic sources in a jet.* Mathematically the forcing term (5.1) is modified to be

$$F(z,r,t) = H(t)\cos\omega t\,\delta\left(\sqrt{|z-(z_0+a(t))|^2 + r^2}\right) \tag{5.6}$$

where

$$a(t) = c\,t \pmod 1 . \tag{5.7}$$

The convection speed c was chosen as .5 of the exit mach number of the jet and the frequency as 1.145.

Analysis of the effect of the forcing term (5.6) on the solution of the system (2.5) is difficult even in the case of no mean flow where the acoustic density ρ satisfies the inhomogenous wave equation. Since the derivation of the wave equation from (2.5), involves taking the time derivatives of the first equation in (2.5), it is clear that the forcing term (5.6) will give rise to a combination of a dipole and a monopole as a

---

* This model was suggested by Lucio Maestrello.

forcing term for the wave equation. If the source convection speed c is reduced and the allowed length of drift in (5.7) increased, one expects a Doppler shift to a new frequency

$$w' = w[1 + c \cdot \cos\theta] \quad . \tag{5.8}$$

This was in fact observed in the case of c very small and a large length of drift.

We then consider more realistic parameters such as $c = .3$ and a drift length of 1. Figure 8 is a plot of the SPL change around circles centered at the origin of the source. The first thing to note is that these plots are very similar to those with no drift. There is a slight deepening of the dip as the axis is approached. This was observed in all tests with the drifting sources. Our results show that this deepening decreases as the convection speed of the sources increases and also that the field at angles close to 90° is basically unchanged.

The fundamental difference due to the convection of the sources is in the periodicity of the solution. Our results indicate that for the parameters of (5.7) the solution oscillates with the original frequency. The amplitude of each peak, however, varies substantially, and the solution exhibits a strong quasi-periodic behavior.

VI. Conclusion

The primitive (i.e. Euler) equations for the acoustic perturbations are solved for both the linearized and non-linear versions in axisymmetric cylindrical coordinates. These equations are inherently more accurate, as

no approximations are made, as compared to the convective wave equation. There is little computational disadvantage in solving the first order system as opposed to solving the time dependent convective wave equation. These equations are suitable for both harmonic time dependence and more complicated temporal behavior.

Boundary conditions have been developed which permit the solution to be computed over severely restricted domains. These conditions are asymptotic in the distance of the artificial cutoff. The approximation (4.5) is easy to implement and allows very little reflection of the outgoing waves into the domain of integration. The boundary conditions coupled with a fourth order numerical method permit the computation of accurate solutions with reasonable grids. The explicit code results in great efficiencies on a vector machine (see [16]).

Solutions generated with a time harmonic source agree closely with previous computations in describing the dip in pressure near the axis. Differences away from the axis can probably be attributed to the increased resolution of the present computations. Further results are described with other time-dependent sources as pulse type forcing functions and moving sources. These reveal new phenomena which can not be calculated by previous codes. Extensive computations have indicated that the relative SPL level is very stable under large perturbations. In order to distinguish the effect of various sources one must examine the pressure as a function of time. Physical experiments are presently in progress to verify several of the computations presented in this study.

Acknowledgment

We wish to thank Max D. Gunzburger, M. Yousuff Hussaini, Lucio Maestrello, and Alan Wenzel for stimulating discussions and advice on this work.

REFERENCES

[1] Schubert, L. K. 1972 Numerical study of sound refraction by a jet. *J. Acoust. Soc. Am.* 28, 447-463.

[2] Liu, C. H. and Maestrello, L. 1975 Propagation of sound through a real jet flowfield. *AIAA Journal* 13, 66-70.

[3] Mungur, P., Plumblee, H. E., and Doak, P. E. 1974 Analysis of acoustic radiation in a jet flow environment. *Journal of Sound and Vibration*, 36, 21-52.

[4] Fix, G. J. Gunzburger, M. D., and Nicolaides, R. A. 1978 On numerical methods for acoustic problems. *ICASE Report No. 78-15.*

[5] Maestrello, L. 1975 Acoustic energy flow from subsonic jets and their mean and turbulent flow structures. *Thesis, Institute of Sound and Vibration*

[6] Strang, W. G. 1968 On the construction and comparison of difference schemes. *SIAM J. of Numer. Anal.* 5, 506-517.

[7] MacCormack, R. W. 1970 Numerical solution of the interaction of a shock wave with a laminar boundary layer. *Proc. 2nd Intl. Conf. on Numerical Methods in Fluid Dynamics*, Springer-Verlag, *Lecture Notes in Phys.*, Vol. 8, 531-549.

[8] Gottlieb, D. and Turkel, E. 1976 Dissipative two-four methods for time-dependent problems. *Math. Comp.*, 30, 703-723.

[9] Turkel, E. 1978 On the practical use of high order methods for hyperbolic systems, *ICASE Report 78-19.*

[10] Hellwig, G. 1964 *Partial Differential Equations.* Blaisdell Publishing Company, New York.

[11] Bayliss, A. and Turkel, E., Radiation boundary conditions for acoustic problem. In preparation.

[12] Rogers, Joel. Private Communication.

[13] Friedlander, F. G. 1962 On the radiation field of pulse solutions of the wave equation. *Proc. Roy. Soc.* A, 269, 53-65.

[14] Gottlieb, D., Gunzburger, M. and Turkel, E. 1978 On numerical boundary treatment for hyperbolic systems, *ICASE Report 78-13.*

[15] Engquist, B. and Majda, A. 1977 Absorbing boundary conditions for the numerical simulation of waves, *Math. Comp.*, 31, 629-651.

[16] Bayliss, A. and Turkel, E. 1979 Dynamic acoustics on the STAR-100, to appear in *Proc. Third Intl. Symposia on Computer Methods for PDE's*, Lehigh University, Bethlehem, PA.

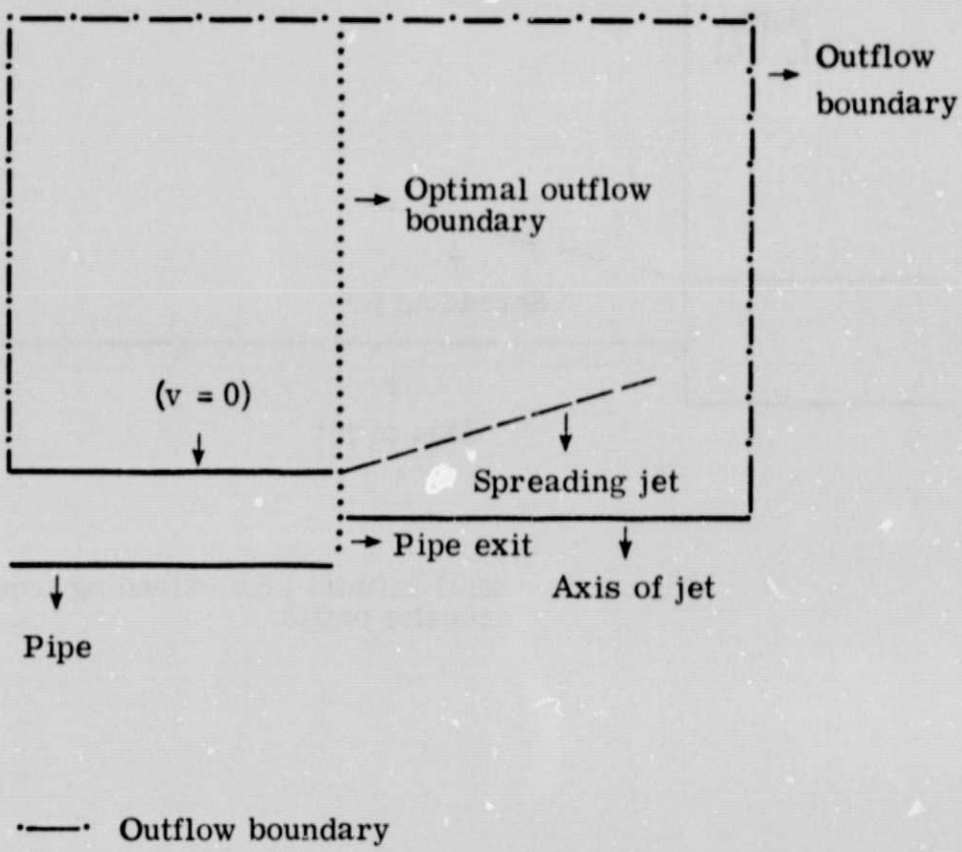

Figure 1. Computational domain for semi-infinite pipe.

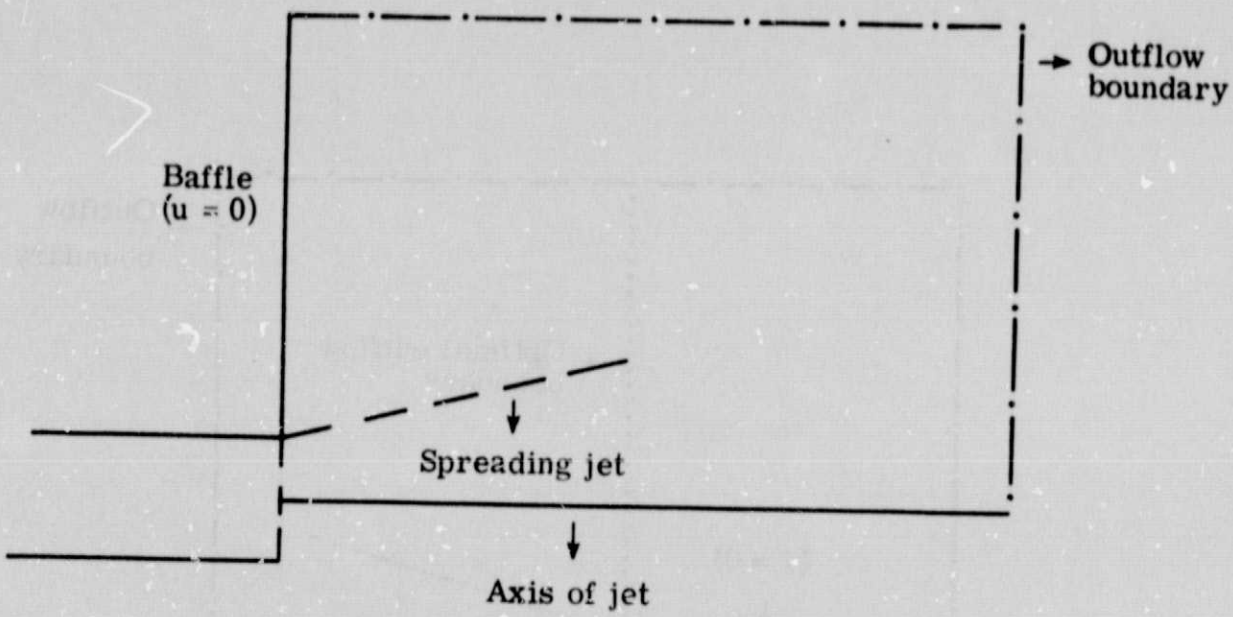

Figure 2. Semi-infinite pipe extending from acoustic baffle.

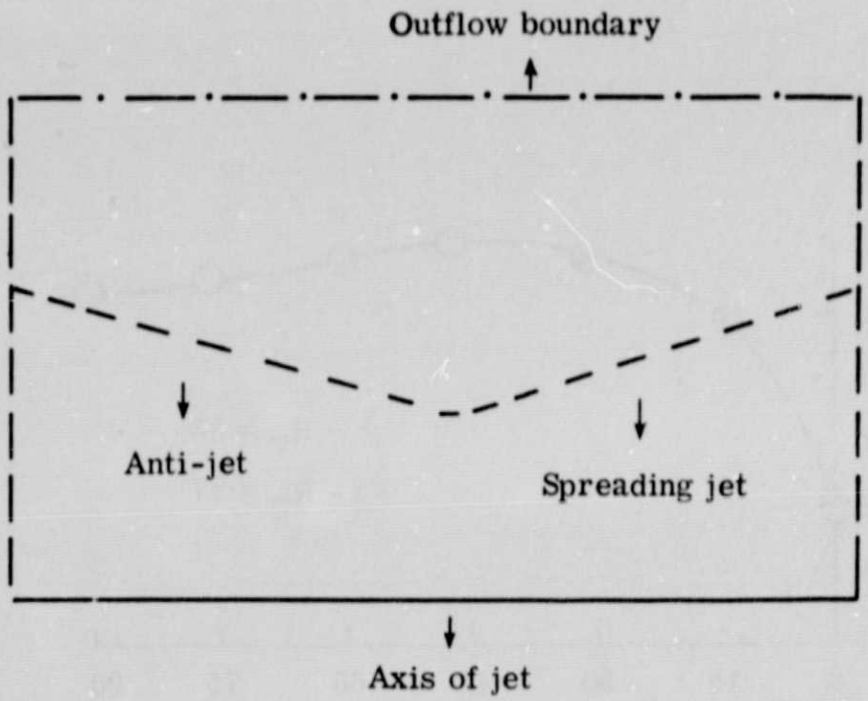

Figure 3. Computational domain for anti-jet configuration.

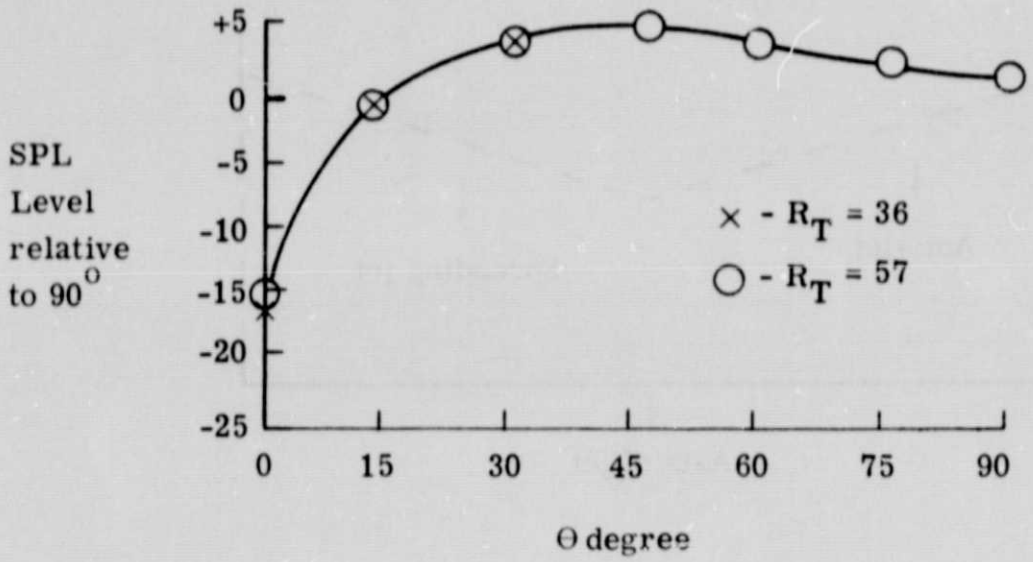

Figure 4a. SPL (relative to 90^{o}) for different values of R_T on a circle 51.4 diameters from source.

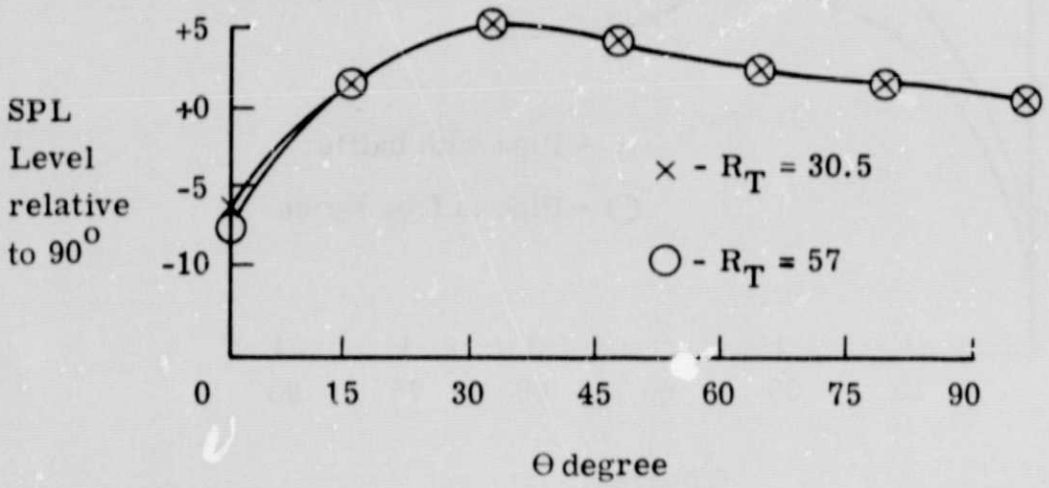

Figure 4b. SPL (relative to 90° for different values of R_T on a circle 19 diameters from source.

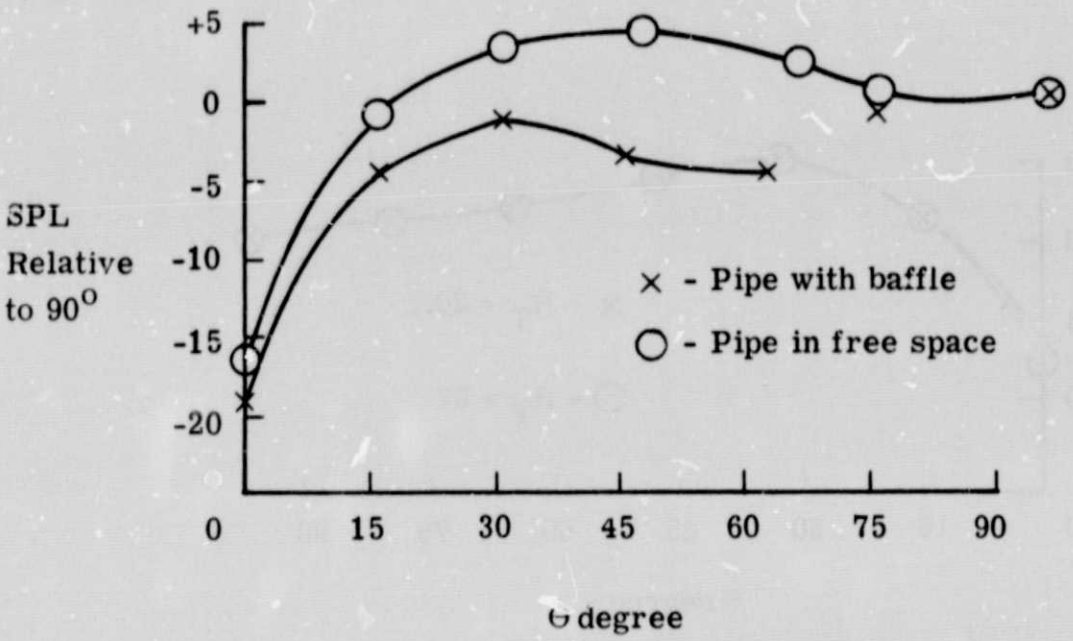

Figure 5. Comparison between jet exiting from a baffle and jet in free space ($\Omega = 1.145$, distance 51.4 diameters from source).

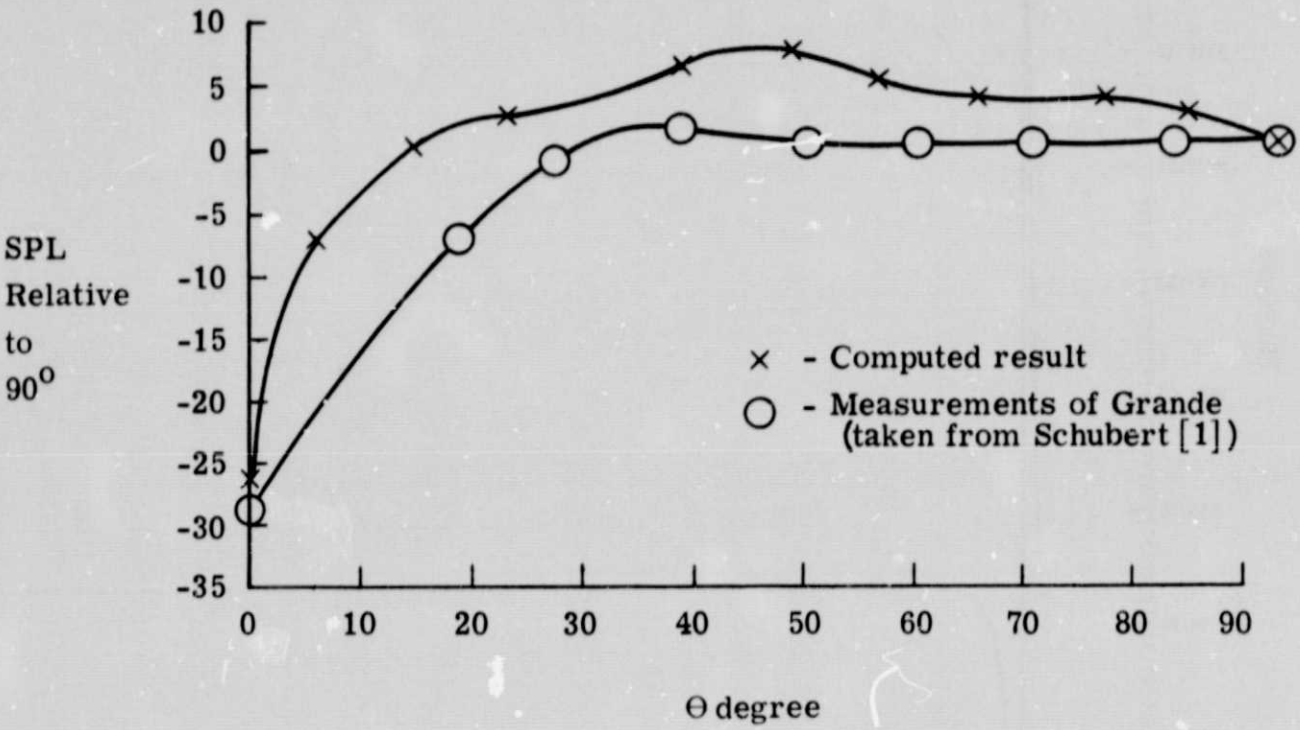

Figure 6. Comparison with experimental results of Grande ($\Omega = 1.055$, Mach number = .9, distance of 100 diameters from source).

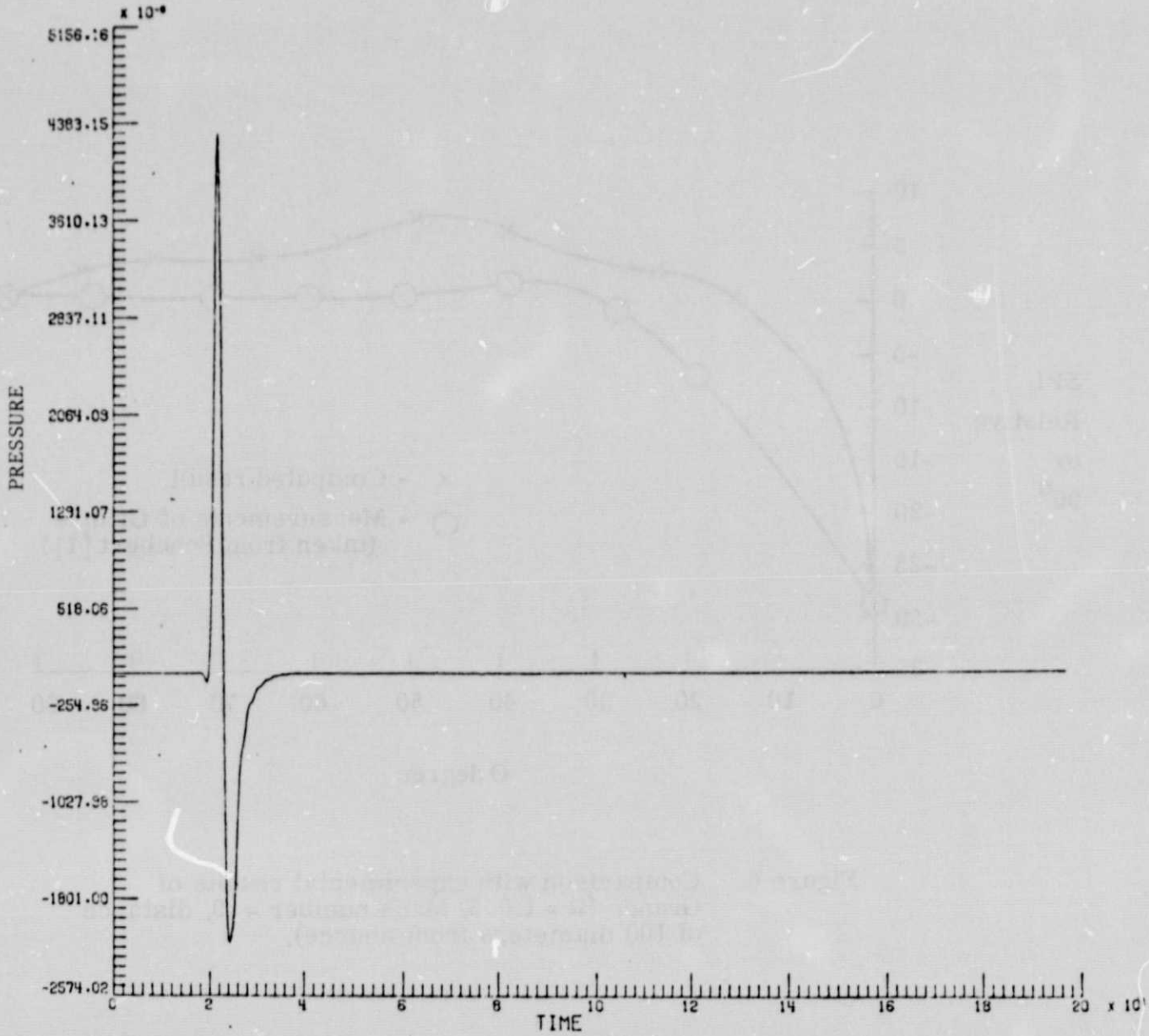

Figure 7a. Pressure from pulse forcing term (Mach number = .01, distance of 20 diameters from source).

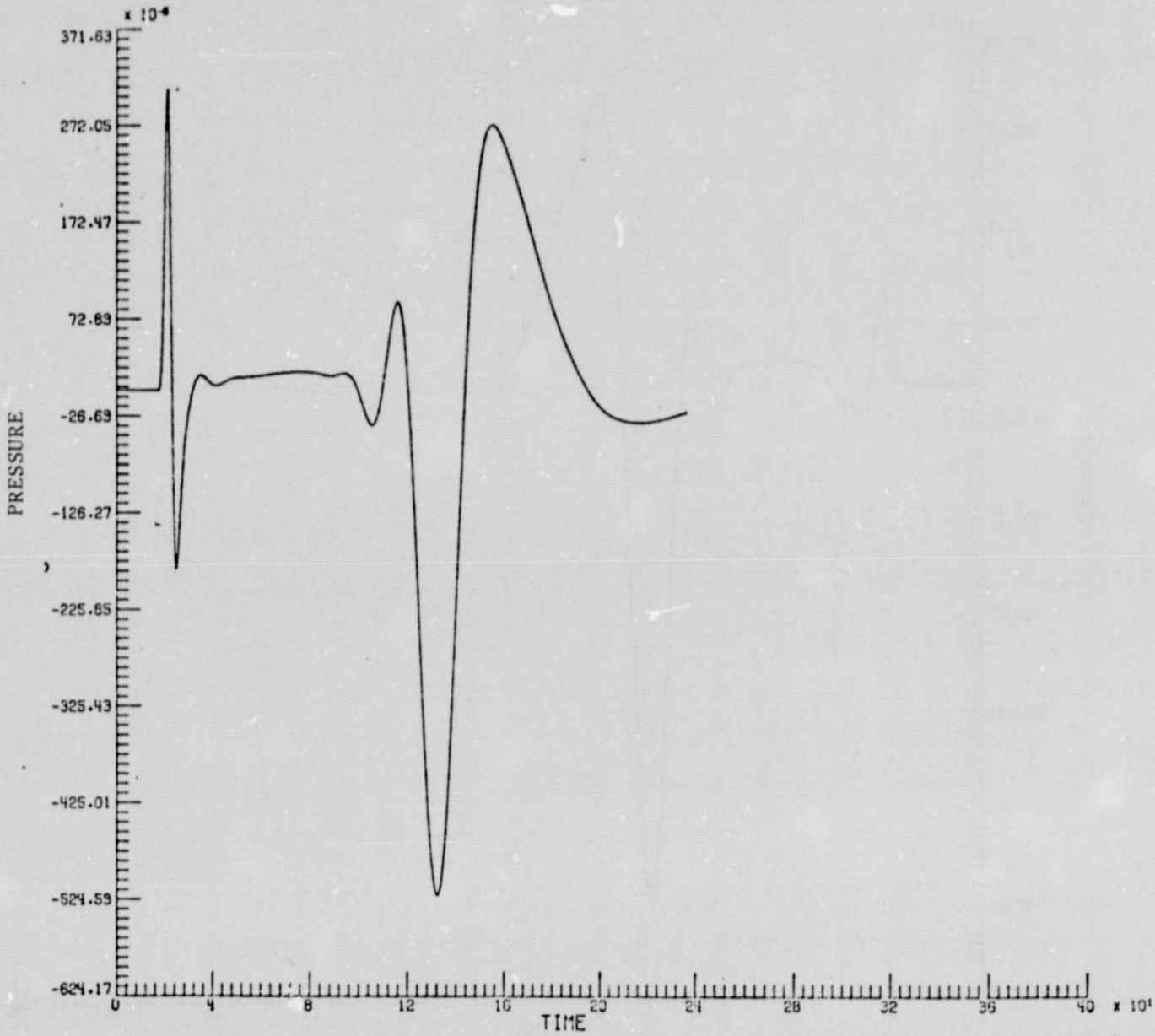

Figure 7b. Pressure from pulse forcing term (Mach number = .31, distance of 20 diameters from source).

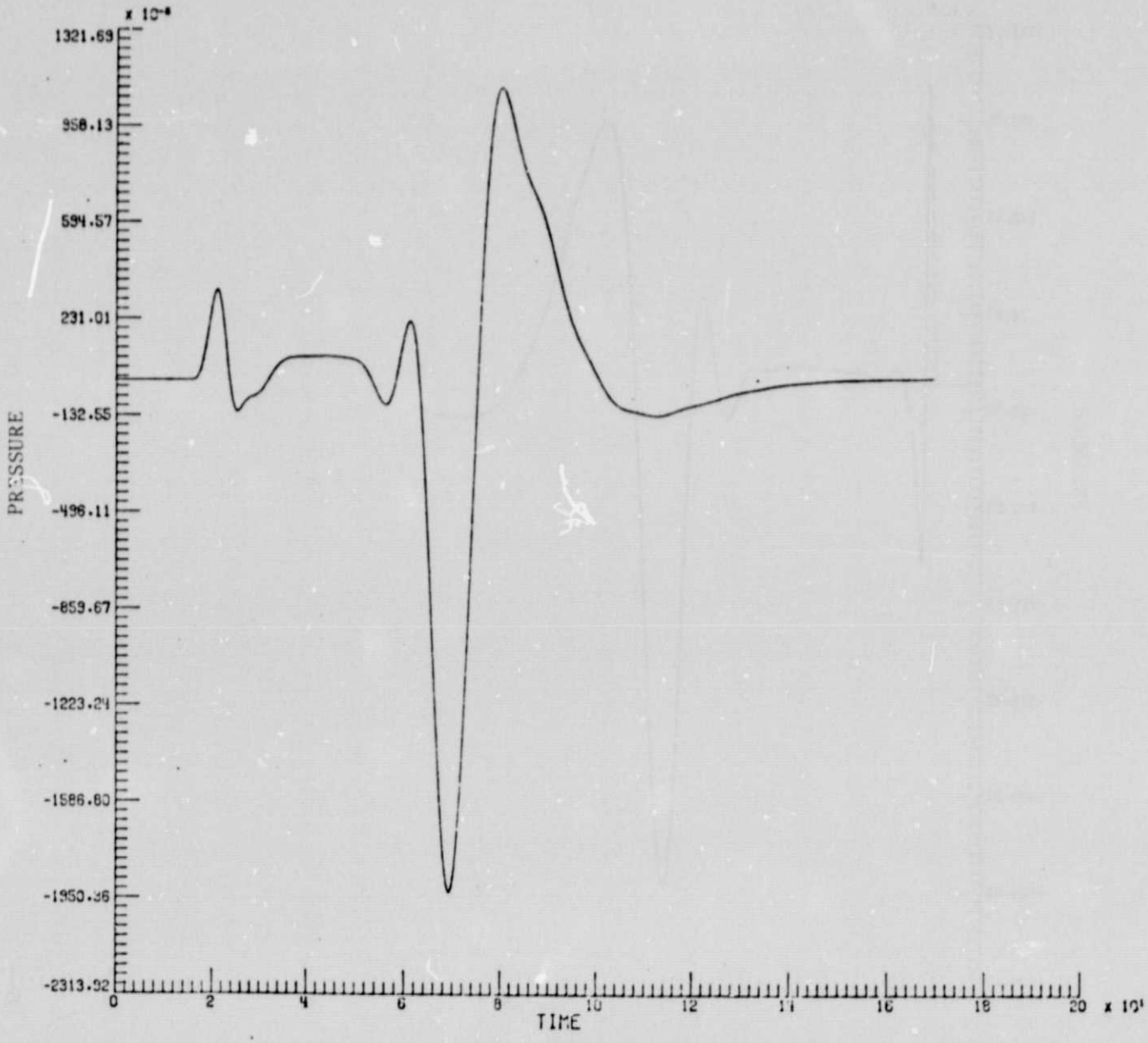

Figure 7c. Pressure from pulse forcing term (Mach number = .62, distance of 20 diameters from source).

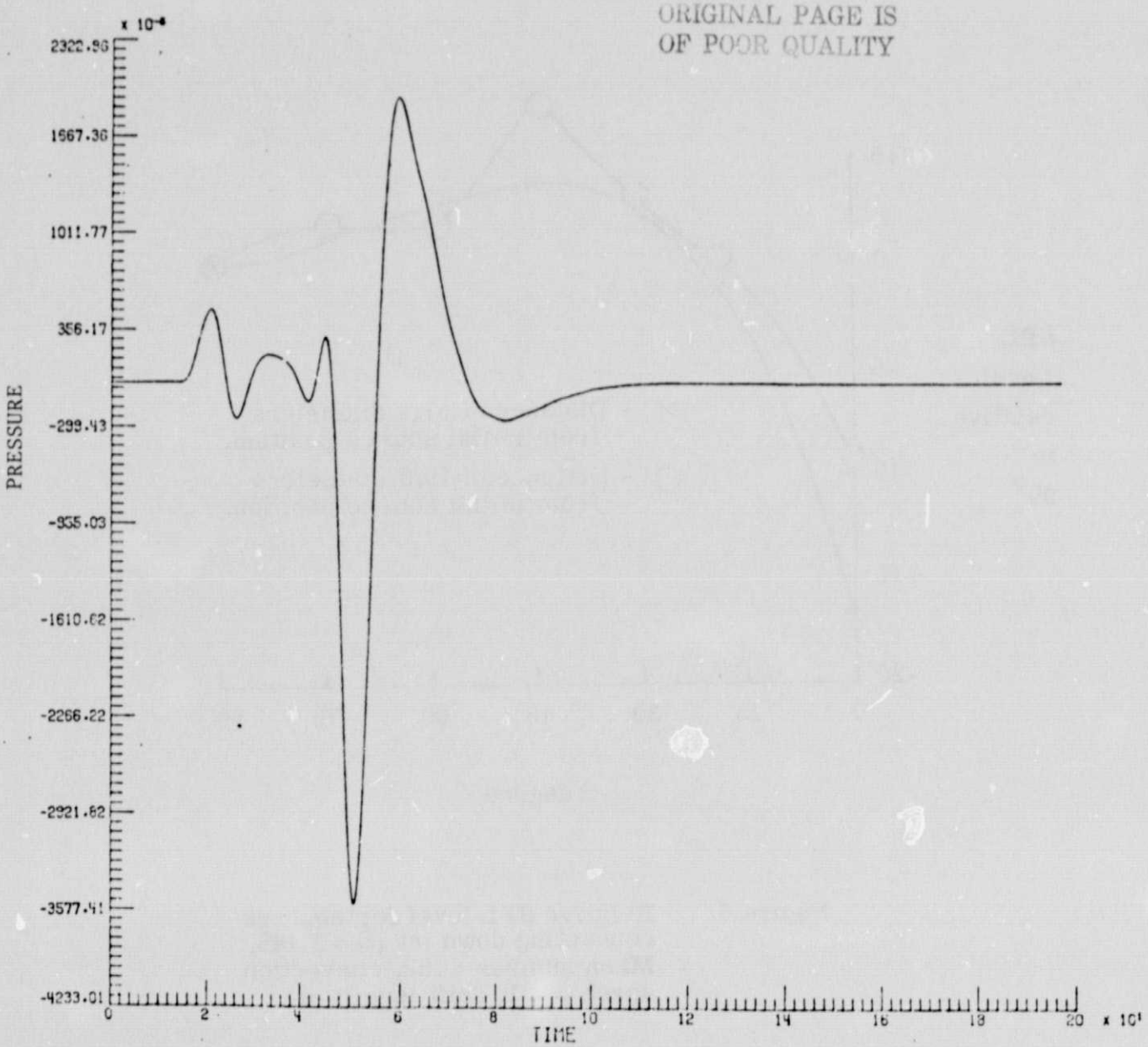

Figure 7d. Pressure from pulse forcing term (Mach number = .85, distance of 20 diameters from source).

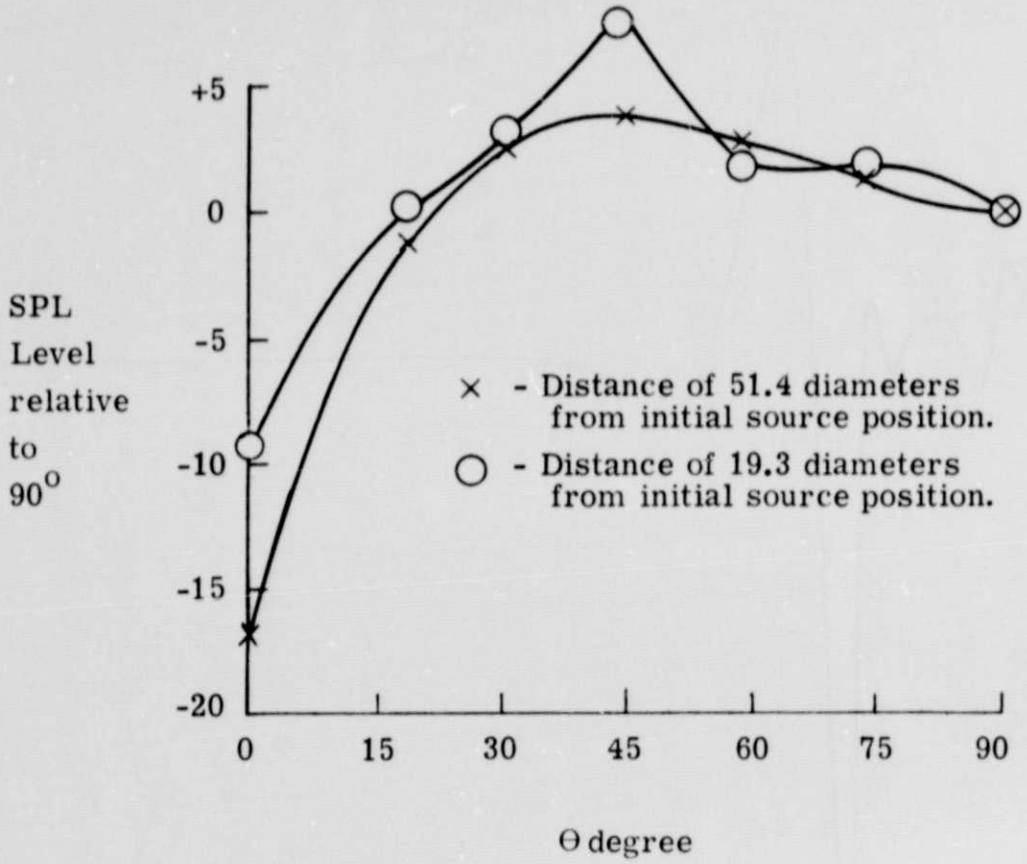

Figure 8. Relative SPL level for sources convecting down jet ($\Omega = 1.145$, Mach number = .62, convection speed = .31, drift length =1).